Disentangling climatic and anthropogenic controls on global terrestrial evapotranspiration trends

2015 Environ. Res. Lett. 10 094008

(http://iopscience.iop.org/1748-9326/10/9/094008)

Environmental Research Letters

CrossMark

OPEN ACCESS

RECEIVED
16 June 2015

REVISED
17 August 2015

ACCEPTED FOR PUBLICATION
18 August 2015

PUBLISHED
8 September 2015

LETTER

Disentangling climatic and anthropogenic controls on global terrestrial evapotranspiration trends

Jiafu Mao[1], Wenting Fu[2], Xiaoying Shi[1], Daniel M Ricciuto[1], Joshua B Fisher[3], Robert E Dickinson[2], Yaxing Wei[1], Willis Shem[1], Shilong Piao[4], Kaicun Wang[5], Christopher R Schwalm[6,7], Hanqin Tian[8], Mingquan Mu[9], Altaf Arain[10], Philippe Ciais[11], Robert Cook[1], Yongjiu Dai[5], Daniel Hayes[1], Forrest M Hoffman[12], Maoyi Huang[13], Suo Huang[10], Deborah N Huntzinger[7,14], Akihiko Ito[15], Atul Jain[16], Anthony W King[1], Huimin Lei[17], Chaoqun Lu[8], Anna M Michalak[18], Nicholas Parazoo[3], Changhui Peng[19], Shushi Peng[11], Benjamin Poulter[20], Kevin Schaefer[21], Elchin Jafarov[21], Peter E Thornton[1], Weile Wang[22], Ning Zeng[23], Zhenzhong Zeng[4], Fang Zhao[23], Qiuan Zhu[19] and Zaichun Zhu[24]

[1] Environmental Sciences Division and Climate Change Science Institute, Oak Ridge National Laboratory, Oak Ridge, TN, USA
[2] Jackson School of Geosciences, the University of Texas, Austin, TX, USA
[3] Jet Propulsion Laboratory, California Institute of Technology, Pasadena, CA, USA
[4] Sino-French Institute for Earth System Science, College of Urban and Environmental Sciences, Peking University, Beijing 100871, People's Republic of China
[5] College of Global Change and Earth System Science, Beijing Normal University, Beijing, People's Republic of China
[6] Center for Ecosystem Science and Society, Northern Arizona University, Flagstaff, AZ 86011, USA
[7] School of Earth Sciences and Environmental Sustainability, Northern Arizona University, Flagstaff, AZ 86011, USA
[8] International Center for Climate and Global Change Research and School of Forestry and Wildlife Sciences, Auburn University, Auburn, AL 36849, USA
[9] Department of Earth System Science, University of California, Irvine, CA, USA
[10] School of Geography and Earth Sciences and McMaster Centre for Climate Change, McMaster University, Hamilton, Ontario, Canada
[11] Laboratoire des Sciences du Climat et de l'Environnement, LSCE, F-91191 Gif sur Yvette, France
[12] Climate Change Science Institute and Computer Science and Mathematics Division, Oak Ridge National Laboratory, Oak Ridge, TN 37831, USA
[13] Atmospheric Sciences and Global Change Division, Pacific Northwest National Laboratory, Richland, WA 99354, USA
[14] Department of Civil Engineering, Construction Management, and Environmental Engineering, Northern Arizona University, Flagstaff, AZ 86011, USA
[15] National Institute for Environmental Studies, Tsukuba, Ibaraki 305-8506, Japan
[16] Department of Atmospheric Sciences, University of Illinois, Urbana, IL 61801, USA
[17] Department of Hydraulic Engineering, Tsinghua University, Beijing 100084, People's Republic of China
[18] Department of Global Ecology, Carnegie Institution for Science, Stanford, CA 94305, USA
[19] Institute of Environmental Sciences, University of Quebec at Montreal (UQAM), Case postale 8888, succ Centre-Ville, Montréal, QC H3C 3P8, Canada
[20] Department of Ecology, Montana State University, Bozeman, MT 59717, USA
[21] National Snow and Ice Data Center, Cooperative Institute for Research in Environmental Sciences, University of Colorado at Boulder, Boulder, CO 80309, USA
[22] Ames Research Center, National Aeronautics and Space Administration, Moffett Field, Mountain View, CA 94035, USA
[23] Department of Atmospheric and Oceanic Science, University of Maryland, College Park, MD 20742, USA
[24] State Key Laboratory of Soil Erosion and Dryland Farming on the Loess Plateau, Northwest A&F University, Yangling 712100, People's Republic of China

E-mail: maoj@ornl.gov

Keywords: evapotranspiration, natural and anthropogenic controls, factorial analysis, MsTMIP

Supplementary material for this article is available online

Abstract

We examined natural and anthropogenic controls on terrestrial evapotranspiration (ET) changes from 1982 to 2010 using multiple estimates from remote sensing-based datasets and process-oriented land surface models. A significant increasing trend of ET in each hemisphere was consistently revealed by observationally-constrained data and multi-model ensembles that considered historic natural and anthropogenic drivers. The climate impacts were simulated to determine the spatiotemporal variations in ET. Globally, rising CO_2 ranked second in these models after the predominant climatic influences, and yielded decreasing trends in canopy transpiration and ET, especially for tropical forests and high-latitude shrub land. Increasing nitrogen deposition slightly amplified global ET via enhanced

plant growth. Land-use-induced ET responses, albeit with substantial uncertainties across the factorial analysis, were minor globally, but pronounced locally, particularly over regions with intensive land-cover changes. Our study highlights the importance of employing multi-stream ET and ET-component estimates to quantify the strengthening anthropogenic fingerprint in the global hydrologic cycle.

1. Introduction

Intensified global hydrological cycle has been observed and modeled during the past few years (Huntington 2006, Gerten *et al* 2008, Wang *et al* 2010, Durack *et al* 2012, Douville *et al* 2013, Sterling *et al* 2013, Wu *et al* 2013, Gedney *et al* 2014). Terrestrial evapotranspiration (ET) is arguably the central component of this changing hydrologic cycle, and functions as a vital link between energy, water and carbon cycles, thereby having important implications for the availability and usage of fresh water resources by humans and terrestrial ecosystems (Seneviratne *et al* 2006, Trenberth *et al* 2009, Fisher *et al* 2011, Wang and Dickinson 2012).

Natural environmental factors (e.g. precipitation, temperature, incident solar radiation, soil moisture, wind and atmospheric teleconnections) regulate ET and its variability across different terrestrial ecosystems (Teuling *et al* 2009, Jung *et al* 2010, Wang *et al* 2010, Vinukollu *et al* 2011, Zhang *et al* 2012, Miralles *et al* 2014). These natural controls and limitations/co-limitations of ET are scale-dependent. Their mechanistic understanding is very important to predict the tendency and variability of ET (Wang and Dickinson 2012). Human-induced land use/land cover change, ground water withdrawals, and irrigation can directly alter the amount and timing of ET by modifying the local water and energy balances (Piao *et al* 2007, Gerten 2013, Leng *et al* 2013, 2014a, 2014b, Lo and Famiglietti 2013, Sterling *et al* 2013, Lei *et al* 2014c). Human activities that contribute to greenhouse gas emissions, atmospheric nitrogen deposition (NDE), and ozone pollution can also alter ET indirectly through changes in physiological, structural and compositional responses of plants (Gedney *et al* 2006, Betts *et al* 2007, Sitch *et al* 2007, Cao *et al* 2009, Leakey *et al* 2009). Discriminating these anthropogenic perturbations from natural factors is expected to increase in importance as anthropogenic transformation of the Earth System becomes more pervasive (Seneviratne *et al* 2010, Gerten 2013).

Based on mechanistic and empirical algorithms that are driven by remotely sensed observations, a variety of globally gridded diagnostic ET products have been compiled and evaluated in recent years (Willmott *et al* 1985, Fisher *et al* 2008, Jiménez *et al* 2009, Jung *et al* 2009, Sheffield *et al* 2010, Zhang *et al* 2010b, Miralles *et al* 2011, Mueller *et al* 2011, Vinukollu *et al* 2011, Zeng *et al* 2012, Schwalm *et al* 2013). These gridded ET estimates offer crucial sources and benchmarks for quantitative investigations of historical ET dynamics over the land surface. However, the accuracy of these observation-based ET products has yet to be reconciled due to limitations in underlying hypotheses and errors in input datasets (Mueller *et al* 2011, 2013, Polhamus *et al* 2012). Moreover, due to their reliance on the satellite observations, these datasets offer a limited historical temporal record that encompasses only a few decades (Badgley *et al* 2015).

To predict future changes in ET patterns, process-based simulation and understanding of the magnitudes, mechanisms and interactions that control historical ET dynamics will be required and should be within uncertainty of both historical and present-day observations. Mechanistic land surface models (LSMs), driven by measurement-based environmental properties, are useful tools for the detection and attribution of natural and anthropogenic effects on ET dynamics. For the past decade, global factorial LSM experiments have been conducted and analyzed by different modeling groups to investigate the separate effects of environmental stresses on land surface and subsurface runoff, river flow, ET and water use efficiency (Gedney *et al* 2006, 2014, Piao *et al* 2007, Shi *et al* 2011, 2013, Tian *et al* 2011, Liu *et al* 2012, Tao *et al* 2014). The role of climate impacts on these hydrologic variables has been characterized predominantly across different regions of the globe. The relative role of natural environmental change versus anthropogenic activities, however, was modeled to be heterogeneous and geographically dependent. Nevertheless, due to large differences in initial model conditions, driver data, and complex parameterizations that govern models, the simulated ET was demonstrated to vary in magnitudes and responses across models at both temporal and spatial scales (Wang *et al* 2010).

To disentangle these differences in simulated ET patterns and the relative role of model sensitivity and structure, the experimental setup and boundary/initial data must be similar among different participating models. We leveraged the controlled factorial experiments and model simulation protocol from the Multi-Scale Synthesis and Terrestrial Model Intercomparison Project (MsTMIP) (Huntzinger *et al* 2013). Further, we synthesized a global ET time series (1982–2010) based on a diverse set of diagnostic ET products (table 1), and the methodology reported recently in Mueller *et al* (2013). The partitioning of ET

Table 1. Overview of the diagnostic ET datasets used for the merged ET of this study, and the simulated ET from MsTMIP models. Factorial results of the MsTMIP multi-model are ALL: the impact from all historical forcing factors, CLI: the impact from historical climate only, OTH: all anthropogenic impacts, CO_2: the historical CO_2 impact only, NDE: the historical nitrogen deposition impact only, LUC: the historical land use/land cover change impact only, Y: the availability of ET simulation for the particular impact, and N: the non-availability of ET simulation for the particular impact.

Group	Name	Algorithm	Spatial resolution	Precipitation data	Time period	Citation
Diagnostic ET	GLEAM	Modified Priestley–Taylor	0.25° × 0.25°	GPCP CMORPH	1982–2010	Miralles *et al* (2011)
	CSIRO	Modified Penman–Monteith	0.5° × 0.5°	SILO	1984–2005	Zhang *et al* (2010b)
	MPI	Empirically derived from FLUXNET	0.5° × 0.5°	GPCC	1982–2008	Jung *et al* (2009)
	NTSG	Modified Penman–Monteith	0.5° × 0.5°	GPCC	1983–2006	Zhang *et al* (2010a)
	PRUNI (3 sets of data)	Penman–Monteith/Priestley–Taylor (ISCCP, AVHRR, SRB)	0.25° × 0.25°	Sheffield *et al* (2006)	1984–2007	Sheffield *et al* (2010)
	PT-JPL	Modified Priestley–Taylor	0.5° × 0.5°	Not required	1984–2006	Fisher *et al* (2008)
	UDEL	Modified Thornthwaite water budget	0.5° × 0.5°	GHCN2	1980–2008	Willmott *et al* (1985)
	PUB	Empirical method (TWSA, CRU)	0.5° × 0.5°	GRACE	1982–2009	Zeng *et al* (2012)
	AWB	Water balance	0.5° × 0.5°	GPCP	1990–2006	Mueller *et al* (2011)

Group	Name	Algorithm	Spatial Resolution		Time Period	Citation	CLI	LUC	CO_2	NDE	ALL	OTH
MsTMIP ET	CLM4	Modified Penman–Monteith	0.5° × 0.5°	CRUNCEP	1982–2010	Lawrence *et al* (2007), Mao *et al* (2012)	Y	Y	Y	Y	Y	Y
	DLEM	Penman–Monteith	0.5° × 0.5°	CRUNCEP	1982–2010	Tian *et al* (2011, 2012)	Y	Y	Y	Y	Y	Y
	BIOME-BGC	Penman–Monteith	0.5° × 0.5°	CRUNCEP	1982–2010	Thornton *et al* (2002)	Y	N	N	N	Y	Y
	CLASS-CTEM-N+	Modified Penman–Monteith	0.5° × 0.5°	CRUNCEP	1982–2010	Huang *et al* (2011), Bartlett *et al* (2006)	Y	Y	Y	Y	Y	Y
	CLM4-VIC	Modified Penman–Monteith	0.5° × 0.5°	CRUNCEP	1982–2010	Lei *et al* (2014a)	Y	Y	Y	Y	Y	Y
	ISAM	Modified Penman–Monteith	0.5° × 0.5°	CRUNCEP	1982–2010	Jain *et al* (1996)	Y	Y	Y	Y	Y	Y
	LPJ-WSL	Modified Penman–Monteith	0.5° × 0.5°	CRUNCEP	1982–2010	Sitch *et al* (2003)	Y	Y	Y	N	Y	Y
	ORCHIDEE-LSCE	Modified Penman–Monteith	0.5° × 0.5°	CRUNCEP	1982–2010	Krinner *et al* (2005)	Y	Y	Y	N	Y	Y
	SiB3-JPL	Penman–Monteith	0.5° × 0.5°	CRUNCEP	1982–2010	Baker *et al* (2008)	Y	Y	Y	N	Y	Y
	SiBCASA	Penman–Monteith	0.5° × 0.5°	CRUNCEP	1982–2010	Schaefer *et al* (2008, 2009)	Y	Y	Y	N	Y	Y
	TRIPLEX-GHG	Modified Penman–Monteith	0.5° × 0.5°	CRUNCEP	1982–2010	Peng *et al* (2011)	N	N	Y	Y	Y	N
	VEGAS	Bulk transfer formula	0.5° × 0.5°	CRUNCEP	1982–2010	Zeng *et al* (2005)	Y	Y	Y	N	Y	Y
	VISIT	Penman–Monteith	0.5° × 0.5°	CRUNCEP	1982–2010	Ito and Inatomi (2012)	Y	Y	Y	N	Y	Y

(e.g canopy transpiration (Tr) and evaporation from wet canopy and bare soil (ET–Tr)) and the variation of those ET components are poorly understood and less constrained by observations (Lawrence *et al* 2007, Jasechko *et al* 2013, Swenson and Lawrence 2014, Wang *et al* 2014). The MsTMIP modeling framework can advance our understanding of trends in ET by providing predictions of the individual ET components. In this study, we thus further investigated the contribution of individual influencing factors to the spatial and temporal characteristics of these ET constituents.

2. Datasets and methods

We created a merged diagnostic ET data (DIA) from 11 long-term diagnostic datasets, all based on different assumptions and constrained with extensive *in situ* observations or satellite retrievals or both (table 1). We remapped the monthly raw datasets from their original spatial resolutions to the half-degree resolution of the model output from 1982 through 2010 based on data availability. Following Mueller *et al* (2013), we applied both physical and statistical constraints for quality control and bias corrections. For the physical constraint, we developed a dataset of seasonal net radiation maxima using the surface radiation budget (SRB3.0) datasets (Gupta 1983). We then excluded grid points with values exceeding net radiation maxima by more than 25%. The outliers were identified as values that exceed ± 3 standard deviations (Weedon 2011). Then the median values of these quality-controlled multiple ET estimates were treated as the merged product, and were comprehensively compared with the LSM results in this study. As shown in figure S1, the annual anomalies of the previously synthesized ET in Mueller *et al* (2013) are well within the spread of this newly-merged diagnostic data product. This updated product however, provides longer-term dynamics and is more amenable for studies at multi-decadal timescales.

To isolate the contributions of environmental drivers to multi-year ET variations, we utilized the factorial ET simulations from the MsTMIP data archive. Driven by the same environmental forcing (climate variability and trends, rising atmospheric CO_2 concentrations causing fertilization and reducing stomatal opening, nitrogen deposition, land use/land cover change, and soil texture and vegetation types), these state-of-the-art LSMs were employed to identify the principal drivers of interannual variability and multi-decadal changes of ET. Because the evaporation component for canopy and soil, and the snow sublimation, were not separately archived in the standard model outputs in the MsTMIP I protocol (Huntzinger *et al* 2013, 2015), we included all relevant available outputs, namely the ET, Tr and the total evaporation (ET–Tr). Four model experiments: (1) SG1 (time varying climate), (2) SG2 (time-varying climate and land use change history), (3) SG3 (time-varying climate, land use, and atmospheric CO_2), and (4) BG1 (time-varying climate, land-use, atmospheric CO_2 and nitrogen deposition), were analyzed to quantify the effects of each environmental forcing factor on the study variables for the years 1982 through 2010. The transient simulations began in 1901, turning on one time-varying driver at a time. Simulations BG1 or SG3 were used to address the combined impacts from various historical forcing agents for models with (BG1) or without (SG3) an explicit nitrogen cycle. Simulation or simulation differencing was used to quantify the contribution to ET and ET component changes from climate change (CLI) (derived from SG1), land use/land cover change (LUC) (derived from SG2-SG1), rising atmospheric CO_2 (CO_2) (derived from SG3-SG2), NDE (derived from BG1-SG3), or all forcing (ALL) (derived from BG1 or SG3) (table 1). To account for the overall effects from human activity (OTH), we derived the human-induced ET to be the difference between the BG1 and SG1 or SG3 and SG1 simulations.

Annual cropland area and total *tree* coverage information for the 1982–2010 period were derived from the merged product of the SYNergetic land cover MAP (Jung *et al* 2006) and the annual time series of the land use harmonization data (Hurtt *et al* 2011). Additional details on the aforementioned driver data and experimental design can be found in Wei *et al* (2014a, 2014b) and Huntzinger *et al* (2013, 2015).

Growing season ET generally dominates the annual sum over the vegetated area of land (Wang *et al* 2007). We focused our analysis on growing season ET for all observational and modeled data. The dynamic annual growing season information, used to mask the monthly ET between 1982 and 2010, was first determined from the global inventory modeling and mapping studies normalized difference vegetation index (NDVI3g) dataset (Pinzon and Tucker 2014) using a Savitzky–Golay filter (Chen *et al* 2004, Jonsson and Eklundh 2004). It was then refined by excluding the freeze period identified by the Freeze/Thaw Earth System Data Record (Kim *et al* 2011, 2012). In particular, the growing season of tropical rainforests was set to 12 months and it started in January.

3. Results

Across the globe, statistically significant increasing trends of ET were recorded from 1982 to 2010 in the observation-based ET estimates (DIA) (1.18 mm yr^{-2}) and modeled ET from the ALL simulation (0.93 ± 0.31 mm yr^{-2}) (figures 1 and S2, and table S1). Significantly positive annual correlations between the simulated ALL ET and the observed ET were obtained, particularly in the Northern hemisphere (NH) (Land: $R^2 = 0.58$, $p < 0.01$, NH: $R^2 = 0.72$,

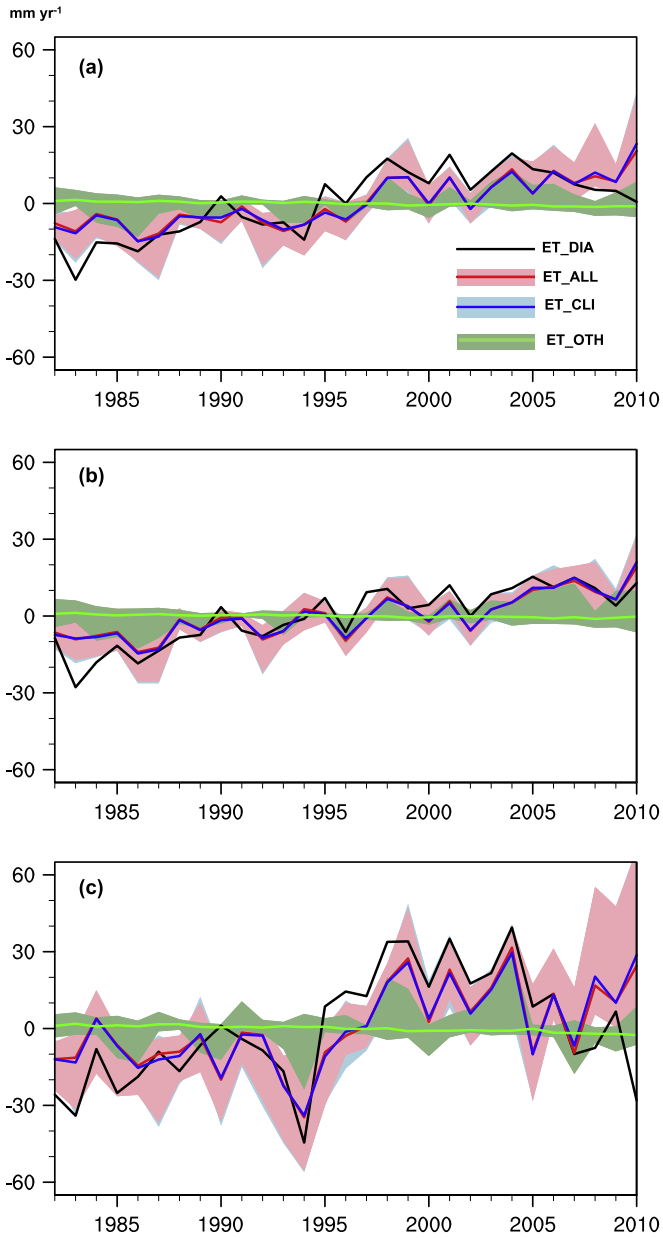

Figure 1. Time series of annual anomalies of growing season ET (mm yr^{-1}) over (a) the globe, (b) the NH, and (c) the SH from 1982 to 2010. Solid lines are the median values of the merged ET (ET_DIA, black), MsTMIP ET of ALL (ET_ALL, red), CLI (ET_CLI, blue), and OTH (ET_OTH, green). Shaded areas indicate the ET range of independent MsTMIP models.

$p < 0.01$, and the Southern hemisphere (SH): $R^2 = 0.46$, $p < 0.01$). The simulated multiyear increasing trend and interannual variability of the ALL ET were mainly explained by the CLI ET. In contrast, the overall human-induced OTH ET was predicted to decrease somewhat, and to exhibit relatively small interannual variations.

Spatial analysis of linear trends of ET for the merged observation product revealed remarkably consistent increasing tendency over most continents (figure 2(a)). Local hotspots of reduced ET were diagnosed to occur in the arid regions of Western North America, central Africa, Northern China and Southeastern Asia. By contrast, the modeled changes of ALL ET underestimated the magnitude of ET changes in Eastern North America and Western Europe, and missed the ET decreases in central Africa. But the placement of increasing or decreasing trends in ALL ET largely agreed favorably with those of the observed ET trends, indicating the suitability of examining multiyear ET trends using the all-factor simulations.

Spatial patterns of ET changes that are consistent between the ALL and CLM estimates confirm the dominance of climate forcing in explaining annual ET trends (figures 2(b), (c) and 3(a)). This dominant climatic response of ET trends was chiefly associated with concurrent annual precipitation changes (spatial $R^2 = 0.34$ for ALL ET and precipitation trend, and spatial $R^2 = 0.30$ for CLI ET and precipitation trends, respectively, $P < 0.01$), and tended to show large

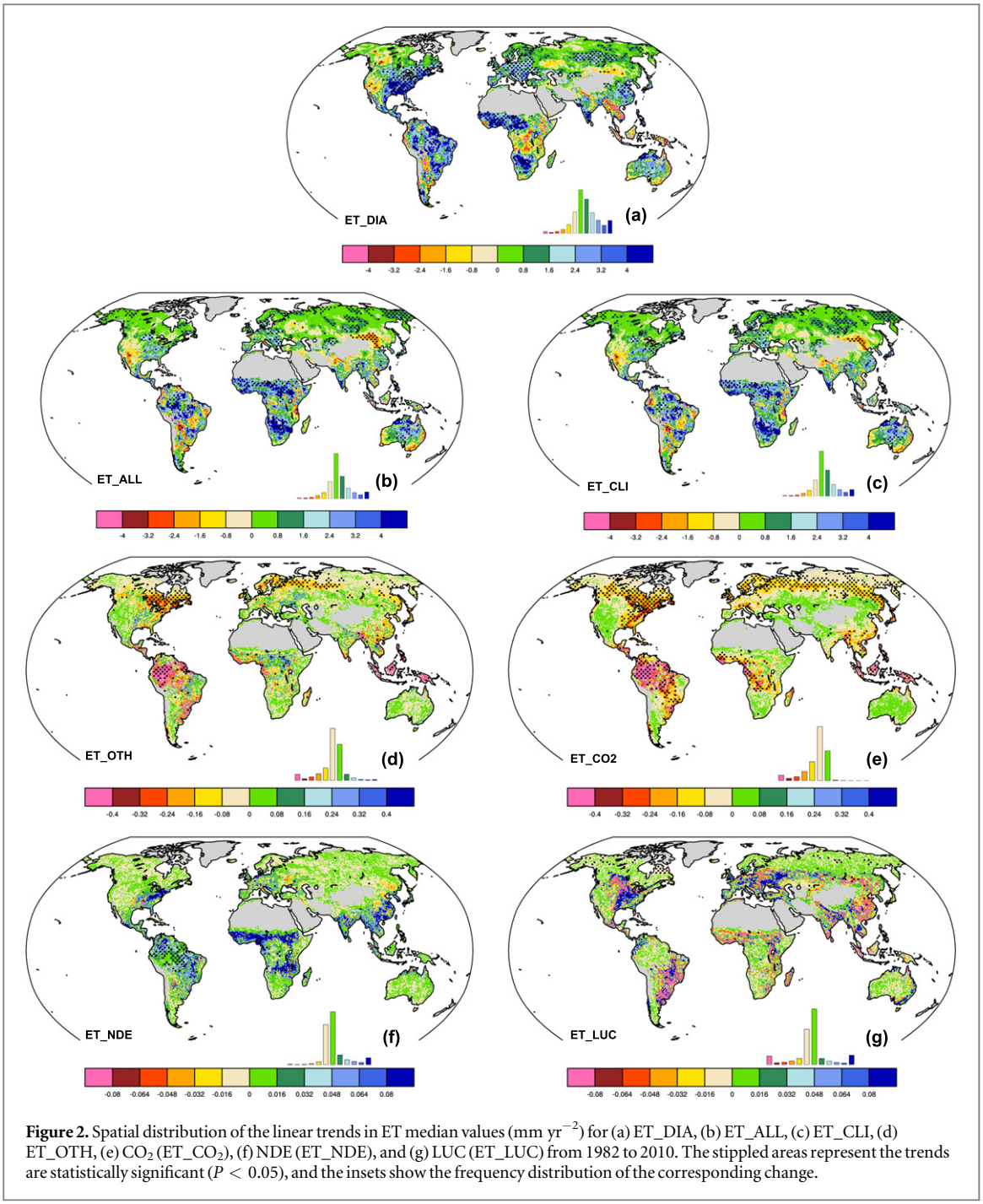

Figure 2. Spatial distribution of the linear trends in ET median values (mm yr^{-2}) for (a) ET_DIA, (b) ET_ALL, (c) ET_CLI, (d) ET_OTH, (e) CO_2 (ET_CO_2), (f) NDE (ET_NDE), and (g) LUC (ET_LUC) from 1982 to 2010. The stippled areas represent the trends are statistically significant ($P < 0.05$), and the insets show the frequency distribution of the corresponding change.

spatial heterogeneities of sign and magnitude (figure 4(a)). The spatial dominance patterns based on the partial correlations among the total growing season ET, precipitation, temperature and incident solar radiation affirmed that for the MsTMIP models, annual precipitation drove not only the interannual variability of ET, but primarily accounted for the multiyear ET trends over most land areas (figures 4(e) and (f)). Combined anthropogenic effects tended to decrease ET, most notably in Northeastern North America, Western Amazon, Northwestern Europe and tropical Asia (figure 2(d)). These effects were subject primarily to the net physiological and structural impacts of CO_2 concentration on the growth of plants in ecosystems (figures 2(e), 3(d), S2 and S3(a)).

Increasing nitrogen deposition led to increasing leaf area index (LAI) (figures 4(b) and S3(b)), and consequently to enhanced terrestrial ET, particularly over South America, Africa and Southeastern China (figures 2(f) and S2). The areas undergoing strong increase in forest fraction and decrease in cropland fraction, such as in central Eastern North America and central Europe, clearly showed increasing annual ET (figures 2(g), 4(c) and (d)). In contrast, regions with evident loss of trees, such as Eastern China and Southeastern South America, show a downtrend of annual

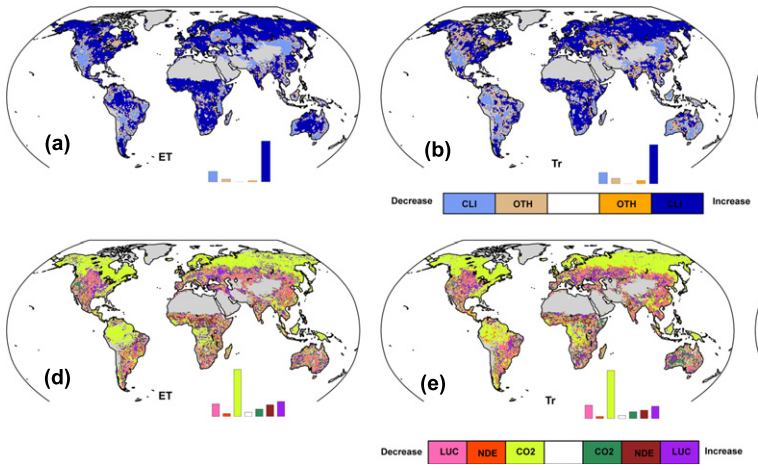

Figure 3. Spatial distribution of the dominant drivers for the ET, Tr and ET–Tr changes for the period 1982–2010. (a)–(c) Dominant drivers for the ET, Tr and ET–Tr trends of the ALL results, and (d)–(f) dominant drivers for the ET, Tr and ET–Tr trends of the OTH results.

ET. Compared to the CO_2 and nitrogen deposition effects, however, the effect of LUC on land ET was important locally. Relatively large uncertainties from the LUC were also found between individual models (figures S2 and S6).

Trends for the Tr and total ET–Tr were dominated by the climatic changes across various continents. For Tr, 85.4% of the study area was impacted by the climatic changes, and 88.7% for ET–Tr (figures 3(b), (c), S4(a)–(f)). Congruent with the response of ET changes to rising CO_2 (48.4 ppm during the period 1982–2010), most areas, especially these regions covered by tropical broadleaf evergreen trees and high latitude shrubs, showed decreasing Tr. This is due to the CO_2-induced reduction in stomatal conductance overwhelming the LAI-induced increase of canopy evaporation and transpiration under elevated CO_2 concentration (figures 3(e) and S4(j)). On the other hand, CO_2 fertilization would enhance canopy LAI through increasing photosynthate allocation to leaves, and caused more canopy transpiration and evaporation than the reduced transpiration by CO_2 physiological effects, especially over dry areas with sparse vegetation (e.g. the Western North America, central Eurasia, and Australia) (figures S3(a) and S4(j)). Reversed ET–Tr trends in these arid regions imply that decreasing soil evaporation was the dominant factor in changing ET–Tr (figures S4(j)–(l)). For most areas that showed decreasing Tr but increasing ET–Tr under CO_2 enrichment, the augmented evaporation of intercepted rainfall and increasing soil evaporation may have been coincidental.

Increasing ET caused by nitrogen deposition was due to enhanced Tr (figures 2(f), S4(m) and S5). A decrease of ET–Tr caused by the nitrogen deposition effect, as seen in central North America and in Western Europe, was due to reduced soil evaporation (figures S4(n) and S5). The latter is a consequence of the increasing LAI providing more shade and so reducing solar energy for soil evaporation. In addition, the increasing Tr further depleted soil water, which reduced soil evaporation. In the evergreen broadleaf forests of the Western Amazon and Congo basin, nitrogen deposition and higher LAI resulted in increasing canopy evaporation. The increase in canopy evaporation more than offset the decrease in soil evaporation and hence dominated the increasing ET–Tr and even the nitrogen-induced increase in total ET (figures S4(m)–(o)).

LUC led to a decreasing trend in Tr across densely inhabited regions that had experienced substantial land use perturbations (e.g. clearing trees for crops) during the study period. These occurred mainly in Southeastern South America and the Eastern China (figures 4(c), (d), S4(p) and S5). Tr trends showed a general negative sign over central Eastern North America and Western Europe, where croplands had been replaced mainly by forests and woodlands. This reduction of Tr with reforestation implies that the tree species that replaced the crops had lower stomatal conductance than the crop species, the younger and smaller trees of the returning forests had lower LAI than the croplands they replaced, or the available soil water for plants decreased because of the removal of irrigation. These aspects deserve further study.

4. Discussion

Between 1982 and 2010, the observation-based and simulated ALL ET consistently showed a significantly increasing trend across the globe. These findings are consistent with previous studies, which reported an intensified global hydrological cycle in response to global warming following the Clausius–Clapeyron law (the relationship between equilibrium water vapor pressure and temperature, about 7% per °C of warming) (Held and Soden 2006), as well as increasing

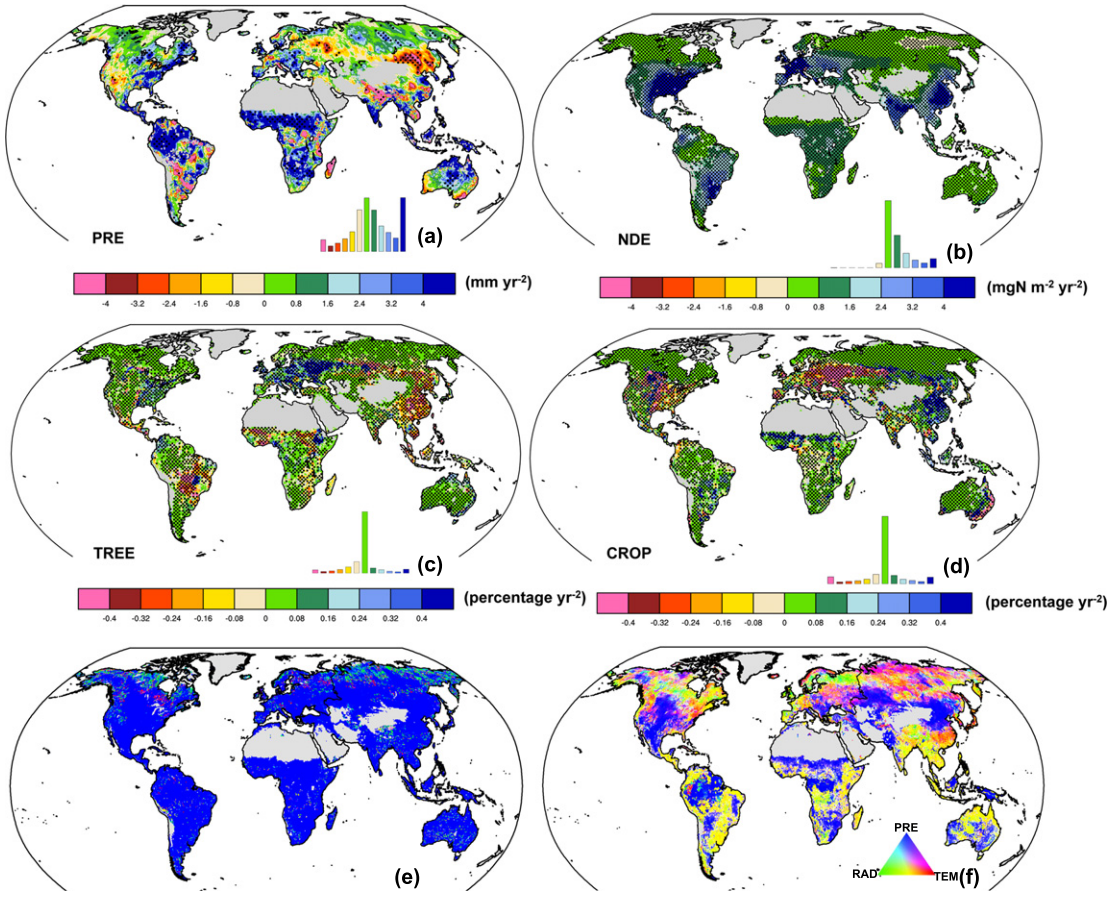

Figure 4. Spatial distribution of trends in (a) precipitation (PRE, mm/yr^{-2}), (b) nitrogen deposition (NDE, mg N m^{-2} yr^{-2}), (c) fractional tree coverage (TREE, %/yr^{-2}), and (d) fractional crop coverage (CROP, %/yr^{-2}) over the period 1982–2010, and spatial distribution of dominant climatic variable (precipitation, temperature (TEM) and incident solar radiation (RAD)) responsible for (e) ET variability, and (f) both variability and trend. For (e), the dominance was derived by comparing the R^2 of the partial correlations between detrended ET and individual climatic factor. For (f), the dominance was derived by comparing the R^2 of the partial correlations between un-detrended ET and individual climatic factor. Both (e) and (f) share the same color legend in (f).

importance of the radiative component of ET (Johnson and Sharma 2010). Climatic factors accounted for much of the spatial and temporal variations in terrestrial ET, Tr and ET–Tr. This supports previous studies regarding the prevalent climatic mechanisms controlling the long-term ET trends such as temperature, precipitation, soil moisture, energy and internal climate variability (Teuling *et al* 2009, Jung *et al* 2010, Wang *et al* 2010, Vinukollu *et al* 2011, Zhang *et al* 2012, Ukkola and Prentice 2013, Miralles *et al* 2014).

In our study, the rising atmospheric CO_2 concentration, as tested by model factorial experiments, induced an overall suppression of Tr and hence a general decreasing ET. Our results further suggest that the sign of change and regional pattern of these CO_2 physiological effects on ET were moderated by changes in LAI. The overall response of ET was eventually determined by the balance among the changes of Tr, canopy evaporation and soil evaporation. These results are consistent with modeled and observed plant physiological responses to the increase of CO_2 concentration in the atmosphere (Betts *et al* 2007, Leakey *et al* 2009). They also reiterate previous findings that show the concurrent physiological and structural responses of vegetation to rising CO_2, and associated hydrological effects (Gedney *et al* 2006, Leipprand and Gerten 2006, Ainsworth and Rogers 2007, Betts *et al* 2007, Kurc and Small 2007, Piao *et al* 2007, Cao *et al* 2009, Leakey *et al* 2009, Lei *et al* 2014b).

Simulation experiments that consider NDE showed enhanced global LAI as a result of increasing nutrient availability (figures 4(b) and S3(b)). The nitrogen-induced enhancement of canopy Tr and canopy evaporation, however, was regionally offset by decreasing soil evaporation, and led to lower ET for the nitrogen fertilization effect. Nonetheless, mineralized nitrogen in the rooting system was governed by not only the amount of deposited N, but also by leaching and denitrification, which are affected by environmental conditions (Hovenden *et al* 2014). This highlights the necessity of better understanding the interactions among these environmental drivers, and the underlying mechanisms responsible for biogeochemical and hydrologic cycles.

Previous modeling *studies* (Boisier *et al* 2012, 2014, Shi *et al* 2013, Sterling *et al* 2013, Tao *et al* 2014) agree with our results that anthropogenic activities modified ET and its components locally, and human-induced LUC effects tended to counteract each other at a global scale. We found large uncertainties associated with LUC impacts among the MsTMIP LSMs, particularly over the NH and areas having marked land cover conversions. Though based on the same merged LUC dataset, different LSM groups prescribed the dynamic evolution of plant functional types with model-specific classifications (Wei *et al* 2014a, 2014b). The sensitivity of biophysical and biogeochemical processes to the reconstructed historical scenario of LUC, moreover, varied considerably from model to model (Huntzinger *et al* 2013). For example, for the SIB3-JPL models, abnormally higher LUC ET was simulated over the NH and global land compared to that of other models (figure S6). In SIB3-JPL, ET is a function of stomatal conductance and is sensitive to changes in photosynthetically active radiation (PAR). In LUC simulations, plant functional type changes over time, but the PAR is prescribed from present day NDVI climatology and is thus fixed to modern vegetation. This can lead to a bias in gross primary production in cases where grasslands are converted to forests, since the NDVI and resulting fraction of incident PAR absorbed by green leaving in the canopy (fPAR) are calculated from a modern day forest ecosystem but used to estimate stomatal conductance and ET for the historical grassland it replaced. The sensitivity to land-use change and cultivated ecosystems (e.g., irrigated croplands) reinforce the need for better LUC characterization, improved parameterization of ET in croplands, and the development of forcing datasets (e.g., PAR) that are not artificially dependent upon land cover. Improvements in these areas may help reduce the large inter-model spreads in the responses of ET to LUC.

Quantitative estimation of ET partitioning has been refined recently, but information on long-term variations and the precise drivers of each ET component are lacking (Jasechko *et al* 2013, Wang *et al* 2014). By using a multi-model ensemble, we assessed the annual trends of the Tr and ET–Tr over nearly three decades, and further estimated their spatial-temporal responses to various environmental stresses. These modeled results, however, remain rather uncertain without observational constrains that are sufficiently long and representative. Comprehensive synthesis of long-term observation-constrained ET components is needed to improve our understanding of the controlling mechanisms, and to better characterize the partitioning schemes.

5. Conclusions

The relative contribution of climate and anthropogenic activities to the spatio-temporal changes in ET was quantitatively characterized with the newly-merged ET and multifactor ensemble simulations from MsTMIP. In the LSMs, climate, CO_2, nitrogen deposition, and land use impacts were separated experimentally to determine the ET variations between 1982 and 2010. Climate, and in particular, changes in precipitation, was the dominant control of multi-year ET trends and variability. The overall CO_2 physiological and structural effect induced decreasing plants transpiration and the total ET, especially in areas where vegetation was dense. Compared to climate change and the elevated CO_2 effects, the impacts of nitrogen deposition and land use change on ET were less important and acted locally. Other detailed explorations are needed, such as the implementation of more compelling statistical techniques and fully-coupled modeling systems (Douville *et al* 2013, Wu *et al* 2013, Gedney *et al* 2014) to detect and attribute the natural and anthropogenic effects on ET with more certainty. ET-related feedback studies are also required to account for land-atmosphere interactions and anthropogenic impacts in the integrated earth system models (Seneviratne *et al* 2010, Bond-Lamberty *et al* 2014, Collins *et al* 2015) and to understand future trajectories of drought (Sheffield *et al* 2012, Zarch *et al* 2015). Given that human activities continue to grow and intensify in the Anthropocene Epoch, we emphasize utilizing multi-stream datasets and multi-modeling frameworks to better diagnose and project anthropogenic influences on terrestrial ET, hydrologic cycle and overall climate change.

Acknowledgments

This research was supported partially by the Terrestrial Ecosystem Science Scientific Focus Area (SFA), which is sponsored by the Terrestrial Ecosystem Science (TES) Program in the Climate and Environmental Sciences Division (CESD) of the Biological and Environmental Research Program in the US Department of Energy Office of Science. This research was supported partially by the Biogeochemistry–Climate Feedbacks SFA and project under contract of DE-SC0012534, which are both sponsored by the Regional and Global Climate Modeling (RGCM) Program in the Climate and Environmental Sciences Division (CESD) of the Biological and Environmental Research Program in the US Department of Energy Office of Science. CRS was supported by National Aeronautics and Space Administration (NASA) Grants #NNX12AP74G, #NNX10AG01A, and #NNX11AO08A. JBF carried out this research at the Jet Propulsion Laboratory, California Institute of Technology, under a contract with NASA. Funding for the Multi-scale synthesis and Terrestrial Model Intercomparison Project (MsTMIP, http://nacp.ornl.gov/MsTMIP.shtml) activity was provided through NASA

ROSES Grant #NNX10AG01A. Data management support for preparing, documenting, and distributing model driver and output data was performed by the Modeling and Synthesis Thematic Data Center at Oak Ridge National Laboratory (ORNL, http://nacp.ornl.gov), with funding through NASA ROSES Grant #NNH10AN681. Finalized MsTMIP data products are archived at the ORNL DAAC (http://daac.ornl.gov). This is MsTMIP contribution #5.

Acknowledgments for specific MsTMIP participating models:

Biome-BGC: *Biome*-BGC code was provided by the Numerical Terradynamic *Simulation* Group at University of Montana. The computational facilities provided by NASA Earth Exchange at NASA Ames Research Center.

CLASS-CTEM-N+: *This* research was funded by the Natural Sciences and Engineering

Research Council (NSERC) of Canada Discovery and Strategic grants. CLASS and CTEM models were originally developed by the Climate Research Branch and Canadian Centre for Climate Modelling and Analysis (CCCMa) of Environment Canada, respectively.

CLM: This research is supported in part by the US Department of Energy (DOE), Office of Science, Biological and Environmental Research. Oak Ridge National Laboratory is managed by UT-Battelle, LLC for DOE under contract DE-AC05-00OR22725.

CLM4VIC: CLM4VIC simulations were supported in part by the US Department of Energy (DOE), Office of Science, Biological and Environmental Research (BER) through the Earth System Modeling program, and performed using the Environmental Molecular Sciences Laboratory (EMSL), a national scientific user facility sponsored by the U.S.DOE-BER and located at Pacific Northwest National Laboratory (PNNL). Participation of M Huang in the MsTMIP synthesis is supported by the U.S.DOE-BER through the Subsurface Biogeochemical Research Program (SBR) as part of the SBR Scientific Focus Area (SFA) at the Pacific Northwest National Laboratory (PNNL). PNNL is operated for the US DOE by BATTELLE Memorial Institute under contract DE-AC05-76RLO1830.

DLEM: The Dynamic Land Ecosystem Model (DLEM) developed in the International Center for Climate and Global Change Research at Auburn University has been supported by NASA Interdisciplinary Science Program (IDS), NASA Land Cover/Land Use Change Program (LCLUC), NASA Terrestrial Ecology Program, NASA Atmospheric Composition Modeling and Analysis Program (ACMAP); NSF Dynamics of Coupled Natural-Human System Program (CNH), Decadal and Regional Climate Prediction using Earth System Models (EaSM); DOE National Institute for Climate Change Research; USDA AFRI Program and EPA STAR Program.

Integrated Science Assessment Model (ISAM) simulations were supported by the US National Science Foundation (NSF-AGS-12-43071 and NSF-EFRI-083598), the USDA National Institute of Food and Agriculture (NIFA) (2011-68002-30220), the US Department of Energy (DOE) Office of Science (DOE-DE-SC0006706) and the NASA Land cover and Land Use Change Program (NNX14AD94G). ISAM simulations were carried out at the National Energy Research Scientific Computing Center (NERSC), which is supported by the Office of Science of the US Department of Energy under contract DE-AC02-05CH11231, and at the Blue Waters sustained-petascale computing, University of Illinois at Urbana- Champaign, which is supported by the National Science Foundation (awards OCI-0725070 and ACI-1238993) and the state of Illinois.

LPJ-wsl: This work was conducted at LSCE, France, using a modified version of the LPJ version 3.1 model, originally made available by the Potsdam Institute for Climate Impact Research.

ORCHIDEE-LSCE: ORCHIDEE is a global land surface model developed at the IPSL institute in France. The simulations were performed with the support of the GhG Europe FP7 grant with computing facilities provided by LSCE (Laboratoire des Sciences du Climat et de l'Environnement) or TGCC (Très Grand Centre de Calcul).

VISIT: VISIT was developed at the National Institute for Environmental Studies, Japan. This work was mostly conducted during a visiting stay at Oak Ridge National Laboratory.

This manuscript has been authored by UT-Battelle, LLC under Contract No. DE-AC05-00OR22725 with the US Department of Energy. The United States Government retains and the publisher, by accepting the article for publication, acknowledges that the United States Government retains a non-exclusive, paid-up, irrevocable, world-wide license to publish or reproduce the published form of this manuscript, or allow others to do so, for United States Government purposes. The Department of Energy will provide public access to these results of federally sponsored research in accordance with the DOE Public Access Plan (http://energy.gov/downloads/doe-public-access-plan).

References

Ainsworth E A and Rogers A 2007 The response of photosynthesis and stomatal conductance to rising (CO_2): mechanisms and environmental interactions *Plant, Cell Environ.* **30** 258–70

Badgley G, Fisher J B, Jiménez C, Tu K P and Vinukollu R 2015 On uncertainty in global evapotranspiration estimates from choice of input forcing datasets *J. Hydrometeorol.* **16** 1449–55

Baker I T, Prihodko L, Denning A S, Goulden M, Miller S and Da Rocha H R 2008 Seasonal drought stress in the amazon: reconciling models and observations *J. Geophys. Res. Biogeo.* **114** 1–10

Bartlett P A, MacKay M D and Verseghy D L 2006 Modified snow algorithms in the Canadian land surface scheme: model runs and sensitivity analysis at three boreal forest stands *Atmos. Ocean* **44** 207–22

Betts R A *et al* 2007 Projected increase in continental runoff due to plant responses to increasing carbon dioxide *Nature* **448** 1037–U5

Boisier J P, de Noblet-Ducoudré N, Pitman A J, Cruz F T, Delire C, van Den Hurk B J J M, van der Molen M K, Mueller C and Voldoire A 2012 Attributing the impacts of land-cover changes in temperate regions on surface temperature and heat fluxes to specific causes: results from the first LUCID set of simulations *J. Geophys. Res. Atmos.* **117** D12116

Boisier J P, de Noblet-Ducoudré N and Ciais P 2014 Historical land-use induced evapotranspiration changes estimated from present-day observations and reconstructed land-cover maps *Hydrol. Earth Syst. Sci. Discuss.* **11** 2045–89

Bond-Lamberty B *et al* 2014 On linking an Earth system model to the equilibrium carbon representation of an economically optimizing land use model*Geosci. Model Devel.* **7** 2545–55

Cao L, Bala G, Caldeira K, Nemani R and Ban-Weiss G 2009 Climate response to physiological forcing of carbon dioxide simulated by the coupled community atmosphere model (CAM3.1) and community land model (CLM3.0) *Geophys. Res. Lett.* **36** 1–5

Chen J, Jonsson P, Tamura M, Gu Z H, Matsushita B and Eklundh L 2004 A simple method for reconstructing a high-quality NDVI time-series data set based on the Savitzky–Golay filter *Remote Sens. Environ.* **91** 332–44

Collins W D *et al* 2015 The integrated Earth system model (iESM): formulation and functionality *Geosci. Model Dev. Discuss.* **8** 381–427

Douville H, Ribes A, Decharme B, Alkama R and Sheffield J 2013 Anthropogenic influence on multidecadal changes in reconstructed global evapotranspiration *Nat. Clim. Change* **3** 59–62

Durack P J, Wijffels S E and Matear R J 2012 Ocean salinities reveal strong global water cycle intensification during 1950–2000 *Science* **336** 455–8

Fisher J B, Tu K P and Baldocchi D D 2008 Global estimates of the land-atmosphere water flux based on monthly AVHRR and ISLSCP-II data, validated at 16 FLUXNET sites *Remote Sens. Environ.* **112** 901–19

Fisher J B, Whittaker R and Malhi Y 2011 ET come home: potential evapotranspiration in geographical ecology *Glob. Ecology Biogeography* **20** 1–18

Gedney N, Cox P M, Betts R A, Boucher O, Huntingford C and Stott P A 2006 Detection of a direct carbon dioxide effect in continental river runoff records *Nature* **439** 835–8

Gedney N, Huntingford C, Weedon G P, Bellouin N, Boucher O and Cox P M 2014 Detection of solar dimming and brightening effects on Northern hemisphere river flow *Nature Geosci.* **7** 796–800

Gerten D 2013 A vital link: water and vegetation in the anthropocene *Hydrol. Earth Syst. Sci.* **17** 3841–52

Gerten D, Rost S, von Bloh W and Lucht W 2008 Causes of change in 20th century global river discharge *Geophys. Res. Lett.* **35** 1–5

Gupta S K 1983 A radiative transfer model for surface radiation budget studies *J. Quant. Spectrosc. Radiat. Trans.* **29** 419–27

Held I M and Soden B J 2006 Robust responses of the hydrological cycle to global warming *J. Clim.* **19** 5686–99

Hovenden M J, Newton P C D and Wills K E 2014 Seasonal not annual rainfall determines grassland biomass response to carbon dioxide *Nature* **511** 583–6

Huang S, Arain M A, Arora V K, Yuan F, Brodeur J and Peichl M 2011 Analysis of nitrogen controls on carbon and water exchanges in a conifer forest using the CLASS-CTEM N+ model *Ecol. Modell.* **222** 3743–60

Huntington T G 2006 Evidence for intensification of the global water cycle: review and synthesis *J. Hydrol.* **319** 83–95

Huntzinger D N *et al* 2013 The North American carbon program multi-scale synthesis and terrestrial model intercomparison project—:1. Overview and experimental design *Geosci. Model Dev.* **6** 2121–33

Huntzinger D N *et al* 2015 *NACP MsTMIP: Global 0.5-deg Terrestrial Biosphere Model Outputs (version 1) in Standard Format* (Tennessee, USA: Oak Ridge National Laboratory Distributed Active Archive Center, Oak Ridge) data set (http://daac.ornl.gov)

Hurtt G C *et al* 2011 Harmonization of land-use scenarios for the period 1500–2100: 600 years of global gridded annual land-use transitions, wood harvest, and resulting secondary lands *Clim. Change* **109** 117–61

Ito A and Inatomi M 2012 Use of a process-based model for assessing the methane budgets of global terrestrial ecosystems and evaluation of uncertainty*Biogeosci.* **9** 759–73

Jain A K, Kheshgi H S and Wuebbles D J 1996 A globally aggregated reconstruction of cycles of carbon and its isotopes *Tellus* B **48** 583–600

Jasechko S, Sharp Z D, Gibson J J, Birks S J, Yi Y and Fawcett P J 2013 Terrestrial water fluxes dominated by transpiration *Nature* **496** 347–50

Jiménez C, Prigent C and Aires F 2009 Toward an estimation of global land surface heat fluxes from multisatellite observations *J. Geophys. Res.* **114** D06305

Jonsson P and Eklundh L 2004 TIMESAT—a program for analyzing time-series of satellite sensor data *Comput. Geosci.* **30** 833–45

Johhnson F and Sharma A 2010 A Comparison of Australian open water body evaporation trends for current and future climates estimated from class A evaporation pans and general circulation models *J. Hydrometeorol.* **11** 105–21

Jung M, Henkel K, Herold M and Churkina G 2006 Exploiting synergies of global land cover products for carbon cycle modeling *Remote Sens. Environ.* **101** 534–53

Jung M, Reichstein M and Bondeau A 2009 Towards global empirical upscaling of FLUXNET eddy covariance observations: validation of a model tree ensemble approach using a biosphere model *Biogeosciences Discuss.* **6** 5271–304

Jung M *et al* 2010 Recent decline in the global land evapotranspiration trend due to limited moisture supply *Nature* **467** 951–4

Kim Y, Kimball J S, McDonald K C and Glassy J 2011 Developing a global data record of daily landscape freeze/thaw status using satellite passive microwave remote sensing *IEEE Trans. Geosci. Remote* **49** 949–60

Kim Y, Kimball J S, Zhang K and McDonald K C 2012 Satellite detection of increasing Northern hemisphere non-frozen seasons from 1979 to 2008: implications for regional vegetation growth *Remote Sens. Environ.* **121** 472–87

Krinner G, Viovy N, de Noblet-Ducoudré N, Ogée J, Polcher J, Friedlingstein P, Ciais P, Sitch S and Prentice I C 2005 A dynamic global vegetation model for studies of the coupled atmosphere–biosphere system *Glob. Biogeochem. Cycles* **19** 1–33

Kurc S A and Small E E 2007 Soil moisture variations and ecosystem-scale fluxes of water and carbon in semiarid grassland and shrubland *Water Resour. Res.* **43** W06416

Lawrence D M, Thornton P, Oleson K W and Bonan G B 2007 The partitioning of evapotranspiration into transpiration, soil evaporation, and canopy evaporation in a gcm: impacts on land–atmosphere interaction *J. Hydrometeorol.* **8** 862–80

Leakey A D B, Ainsworth E A, Bernacchi C J, Rogers A, Long S P and Ort D R 2009 Elevated CO_2 effects on plant carbon, nitrogen, and water relations: six important lessons from FACE *J. Exp. Bot.* **60** 2859–76

Lei H, Huang M, Leung L R, Yang D, Shi X, Mao J, Hayes D J, Schwalm C, Wei Y and Liu S 2014a Sensitivity of global terrestrial gross primary production to hydrologic states simulated by the community land model using two runoff parameterizations *J. Adv. Model. Earth Syst.* **6** 658–79

Lei H, Yang D and Huang M 2014b Impacts of climate change and vegetation dynamics on runoff in the mountainous region of the Haihe River basin in the past five decades *J. Hydrol.* **511** 786–99

Lei H, Yang D, Yang H, Yuan Z and Lv H 2014c Simulated impacts of irrigation on evapotranspiration in a strongly exploited region: a case study of the Haihe River Basin China *Hydrol. Process.* **29** 2704–19

Leipprand A and Gerten D 2006 Content on evapotranspiration, soil moisture and runoff under potential natural vegetation *Hydrol. Sci. J.* **51** 171–85

Leng G, Huang M, Tang Q, Sacks W J, Lei H and Leung L Y R 2013 Modeling the effects of irrigation on land surface fluxes and states over the conterminous United States: sensitivity to input data and model parameters *J. Geophys. Res.-Atmos.* **118** 9789–803

Leng G, Huang M, Tang Q, Gao H and Leung L Y R 2014a Modeling the effects of groundwater-fed irrigation on terrestrial hydrology over the conterminous United States *J. Hydrometeorol.* **15** 957–72

Leng G, Tang Q, Huang M and Leung L R 2014b A comparative analysis of the impacts of climate change and irrigation on land surface and subsurface hydrology in the North China plain *Reg. Environ. Change* **15** 251–63

Liu M, Tian H, Lu C, Xu X, Chen G and Ren W 2012 Effects of multiple environment stresses on evapotranspiration and runoff over Eastern China *J. Hydrol.* **426–7** 39–54

Lo M H and Famiglietti J S 2013 Irrigation in California's central valley strengthens the Southwestern US water cycle *Geophys. Res. Lett.* **40** 301–6

Mao J, Thornton P E, Shi X, Zhao M and Post W M 2012 Remote sensing evaluation of CLM4 GPP for the period 2000–09 *J. Clim.* **25** 5327–42

Miralles D G, Holmes T R H, De Jeu R A M, Gash J H, Meesters A G C A and Dolman A J 2011 Global land-surface evaporation estimated from satellite-based observations *Hydrol. Earth Syst. Sci.* **15** 453–69

Miralles D G *et al* 2014 El Niño–La Niña cycle and recent trends in continental evaporation *Nat. Clim. Change* **4** 122–6

Mueller B *et al* 2011 Evaluation of global observations-based evapotranspiration datasets and IPCC AR4 simulations *Geophys. Res. Lett.* **38** L06402

Mueller B *et al* 2013 Benchmark products for land evapotranspiration: LandFlux-EVAL multi-data set synthesis *Hydrol. Earth Syst. Sci.* **17** 3707–20

Peng C, Ma Z, Lei X, Zhu Q, Chen H, Wang W, Liu S, Li W, Fang X and Zhou X 2011 A drought-induced pervasive increase in tree mortality across Canada's boreal forests *Nat. Clim. Change* **1** 467–71

Piao S, Friedlingstein P, Ciais P, de Noblet-Ducoudré N, Labat D and Zaehle S 2007 Changes in climate and land use have a larger direct impact than rising CO_2 on global river runoff trends *Proc. Natl Acad. Sci. USA* **104** 15242–7

Pinzon J and Tucker C 2014 A non-stationary 1981–2012 AVHRR NDVI3g time series *Remote Sens.* **6** 6929–60

Polhamus A M, Fisher J B and Tu K P 2012 What controls the error structure in evapotranspiration models? *Agric. Forest Meteorol.* **169** 12–24

Schaefer K, Collatz G J, Tans P, Denning A S, Baker I, Berry J, Prihodko L, Suits N and Philpott A 2008 Combined simple biosphere/carnegie-ames-stanford approach terrestrial carbon cycle model *J. Geophys. Res. Biogeo.* **113** G03034

Schaefer K, Zhang T, Slater A G, Lu L, Etringer A and Baker I 2009 Improving simulated soil temperatures and soil freeze/thaw at high-latitude regions in the simple biosphere/carnegie ames-stanford approach model *J. Geophys. Res. Earth Surf.* **114** F02021

Schwalm C R, Huntinzger D N, Michalak A M, Fisher J B, Kimball J S, Mueller B, Zhang K and Zhang Y 2013 Sensitivity of inferred climate model skill to evaluation decisions: a case study using CMIP5 evapotranspiration *Environ. Res. Lett.* **8** 024–8

Seneviratne S I, Lüthi D, Litschi M and Schär C 2006 Land-atmosphere coupling and climate change in Europe *Nature* **443** 205–9

Seneviratne S I, Corti T, Davin E L, Hirschi M, Jaeger E B, Lehner I, Orlowsky B and Teuling A J 2010 Investigating soil moisture–climate interactions in a changing climate: a review *Earth-Science Rev.* **99** 125–61

Sheffield J, Goteti G and Wood E F 2006 Development of a 50-year high-resolution global dataset of meteorological forcings for land surface modeling *J. Climate* **19** 3088–111

Sheffield J, Wood E F and Munoz-Arriola F 2010 Long-term regional estimates of evapotranspiration for Mexico based on downscaled ISCCP data *J. Hydrometeorol.* **11** 253–75

Sheffield J, Wood E F and Roderick M L 2012 Little change in global drought over the past 60 years *Nature* **491** 435–8

Shi X, Mao J, Thornton P E, Hoffman F M and Post W M 2011 The impact of climate, CO_2, nitrogen deposition and land use change on simulated contemporary global river flow *Geophys. Res. Lett.* **38** L08704

Shi X, Mao J, Thornton P E and Huang M 2013 Spatiotemporal patterns of evapotranspiration in response to multiple environmental factors simulated by the community land model *Environ. Res. Lett.* **8** 024012

Sitch S *et al* 2003 Evaluation of ecosystem dynamics, plant geography and terrestrial carbon cycling in the LPJ dynamic global vegetation model *Glob. Change Biol.* **9** 161–85

Sitch S, Cox P M, Collins W J and Huntingford C 2007 Indirect radiative forcing of climate change through ozone effects on the land-carbon sink *Nature* **448** 791–4

Sterling S M, Ducharne A and Polcher J 2013 The impact of global land-cover change on the terrestrial water cycle *Nat. Clim. Change* **3** 385–90

Swenson S C and Lawrence D M 2014 Assessing a dry surface layer-based soil resistance parameterization for the community land model using GRACE and FLUXNET-MTE data *J. Geophys. Res.-Atmos.* **119** 299–312

Tao B, Tian H, Ren W, Yang J, Yang Q, He R, Cai W and Lohrenz S 2014 Increasing Mississippi river discharge throughout the 21st century influenced by changes in climate, land use, and atmospheric CO_2 *Geophys. Res. Lett.* **41** 4978–86

Tian H, Xu X, Lu C, Liu M, Ren W, Chen G, Melillo J and Liu J 2011 Net exchanges of CO_2, CH_4, and N_2O between China's terrestrial ecosystems and the atmosphere and their contributions to global climate warming *J. Geophys. Res. Biogeosci.* **116** G02011

Tian H *et al* 2012 Century-scale responses of ecosystem carbon storage and flux to multiple environmental changes in the Southern United States *Ecosystems* **15** 674–94

Teuling A J *et al* 2009 A regional perspective on trends in continental evaporation *Geophys. Res. Lett.* **36** L02404

Thornton P E *et al* 2002 Modeling and measuring the effects of disturbance history and climate on carbon and water budgets in evergreen needleleaf forests *Agric. For. Meteorol.* **113** 185–222

Trenberth K E, Fasullo J T and Kiehl J 2009 Earth's global energy budget *Bull. Am. Meteorol. Soc.* **90** 311–23

Ukkola A M and Prentice I C 2013 A worldwide analysis of trends in water-balance evapotranspiration *Hydrol. Earth Syst. Sci.* **17** 4177–87

Vinukollu R K, Meynadier R, Sheffield J and Wood E F 2011 Multi-model, multi-sensor estimates of global evapotranspiration: climatology, uncertainties and trends *Hydrol. Process.* **25** 3993–4010

Wang K C, Wang P, Li Z Q, Cribb M and Sparrow M 2007 A simple method to estimate actual evapotranspiration from a combination of net radiation, vegetation index, and temperature *J. Geophys. Res.* **112** D15107

Wang K C, Dickinson R E, Wild M and Liang S 2010 Evidence for decadal variation in global terrestrial evapotranspiration between 1982 and 2002: 2 results *J. Geophys. Res.* **115** D20113

Wang K C and Dickinson R E 2012 A review of global terrestrial evapotranspiration: observation, modelling, climatology, and climatic variability *Rev. Geophys.* **50** RG2005

Wang L, Good S P and Caylor K K 2014 Global synthesis of vegetation control on evapotranspiration partitioning *Geophys. Res. Lett.* **41** 6753–7

Wei Y *et al* 2014a The North American carbon program multi-scale synthesis and terrestrial model intercomparison project: II. Environmental driver data *Geosci. Model Dev.* **7** 2875–93

Wei Y et al 2014b *NACP MsTMIP: Global and North American Driver Data for Multi-Model Intercomparison* (Tennessee, USA: Oak Ridge National Laboratory Distributed Active Archive Center, Oak Ridge) data set (http://daac.ornl.gov)

Willmott C J, Rowe C M and Mintz Y 1985 Climatology of the seasonal terrestrial water cycle *J. Climatol.* **5** 589–606

Wu P, Christidis N and Stott P 2013 Anthropogenic impact on Earth's hydrological cycle *Nat. Clim. Change* **3** 807–10

Zarch M A A, Sivakumar B and Sharma A 2015 Droughts in a warming climate: a global assessment of standardised precipitation index (SPI) and reconnaissance drought index (RDI) *J. Hydrol.* **526** 183–95

Zeng N, Mariotti A and Wetzel P 2005 Terrestrial mechanisms of interannual CO_2 variability *Glob. Biogeochem. Cycles* **19** GB1016

Zeng Z, Piao S, Lin X, Yin G, Peng S, Ciais P and Myneni R B 2012 Global evapotranspiration over the past three decades: estimation based on the water balance equation combined with empirical models *Environ. Res. Lett.* **7** 014026

Zhang K, Kimball J S, Nemani R R and Running S W 2010a A continuous satellite-derived global record of land surface evapotranspiration from 1983 to 2006 *Water Resour. Res.* **46** W09522

Zhang Y, Leuning R, Hutley L B, Beringer J, McHugh I and Walker J P 2010b Using long-term water balances to parameterize surface conductances and calculate evaporation at 0.05° spatial resolution *Water Resour. Res.* **46** W05512

Zhang Y, Leuning R, Chiew F H S, Wang E, Zhang L, Liu C, Sun F, Peel M C, Shen Y and Jung M 2012 Decadal trends in evaporation from global energy and water balances *J. Hydrometeorol.* **13** 379–91